

Topological Orders Beyond Topological Quantum Field Theories

P. Vojta,¹ G. Ortiz,^{2,3} and Z. Nussinov^{4,1,*}

¹*Department of Physics, Washington University in St. Louis, MO 63130 USA*

²*Department of Physics, Indiana University, Bloomington, IN 47405, USA*

³*Institute for Quantum Computing, University of Waterloo, Waterloo, N2L 3G1, ON, Canada*

⁴*Rudolf Peierls Centre for Theoretical Physics, University of Oxford, Oxford OX1 3PU, United Kingdom*

(Dated: December 20, 2023)

Systems displaying quantum topological order feature robust characteristics that are very attractive to quantum computing schemes. Topological quantum field theories have proven to be powerful in capturing the quintessential attributes of systems displaying topological order including, in particular, their anyon excitations. Here, we investigate systems that lie outside this common purview, and present a rich class of models exhibiting topological orders with distance-dependent interacting anyons. As we illustrate, in some instances, *the gapped lowest-energy excitations are comprised of anyons that densely cover the entire system*. This leads to behaviors not typically described by topological quantum field theories. We examine these models by performing dualities to systems displaying conventional (i.e., Landau) orders. Our approach enables a general method for mapping generic Landau-type theories to dual models with topological order of the same spatial dimension. The low-energy subspaces of our models can be made more resilient to thermal effects than those of surface codes.

Introduction. Topological quantum field theories (TQFTs)[1–4], are closely interwoven with existing descriptions of topological quantum order (TQO). Axiomatically, TQFTs are mappings from (inherently metric independent) manifold cobordisms to Hilbert spaces [2]. It is often understood that a microscopic model displaying TQO effectively renormalizes to a certain TQFT in the low-energy limit, resulting in ground-state degeneracies computable via that TQFT [5, 6]. Consequently, many distinct microscopic models may be associated with the same type of TQO. Importantly, from a practical standpoint, the properties of *gapped low-energy (anyon) excitations* in TQO systems are typically analyzed via such TQFTs [7]. These excitations form the focus of our attention.

In this work we report on TQO systems for which conventional TQFT descriptions are insufficient. The interactions in these systems non-trivially alter the braiding and fusion properties of their lowest-energy excitations (these excitations may become unbounded so as to cover all of space) without modifying the ground-state space TQFT. To elucidate the basic premise, we introduce and study simple \mathbb{Z}_q (with $q \geq 2$) extensions of the well-known ($q = 2$) Kitaev toric code (TC) [8] models. As detailed in [9], such extensions apply far more generally to string-net type [10–13], and other models. These TQO models map, via exact dualities, to theories exhibiting Landau orders. Our framework is general and includes theories with long-range interactions and non-abelian degrees of freedom [14] in any number of spatial dimensions.

Diverse, and often inequivalent [15, 16], notions of TQO abound. We follow Kitaev’s definition which highlights the innate robustness of TQO systems to (quasi-) local perturbations [8], hence their promise for topological quantum information processing. According to this error-detection motivated definition, the matrix elements

of all (quasi-)local operators V in the ground-state basis, spanned by orthonormal states $\{|g_\gamma\rangle\}$, satisfy

$$\langle g_\alpha | V | g_\beta \rangle = v \delta_{\alpha,\beta}, \quad (1)$$

with v a constant depending only on V . Physically, Eq. (1) asserts that different ground-states cannot be told apart via (quasi-) local measurements (and thus cannot be assigned different conventional Landau order parameters). Such a condition may be extended beyond the lowest-energy (i.e., ground-state) sector [15, 16]. For symmetry enriched topological order (SET) [17], v may include quantum numbers associated with symmetries.

TQFTs are indispensable in studies of numerous TQO systems where they describe anyon braiding and fusion [7]. With the exception of theories exhibiting rigid subsystem symmetries (e.g., fractons and related models), where the degeneracy increases with system size, [18–25], TQFTs generally encode ground-state (anyon vacuum) degeneracies. We will show that excitations of TQO systems may differ from those of expected anyon models. Even in the infrared limit, whenever (anyon) excitations appear, their salient characteristics will be metric (i.e., geometry) dependent. TQFT descriptions of the vacuum remain unaltered.

The Star-Plaquette Product Model (SPPM). Our primary workhorse will be the “ q -state SPPM.” On general lattices Λ , this model is given by the nearest-neighbor Hamiltonian (see Fig. 1),

$$H_{\text{SPPM}} = - \sum_{\langle s,p \rangle} J_{sp} A_s B_p - \sum_s g_s A_s - \sum_p g_p B_p + \text{h.c.}, \quad (2)$$

defined on a Hilbert space \mathcal{H} formed by the tensor product of N_Λ link subspaces. The $\langle s,p \rangle$ sum in the first term is over neighboring “stars” and “plaquettes” (see left panel of Fig. 1) that share common lattice links.

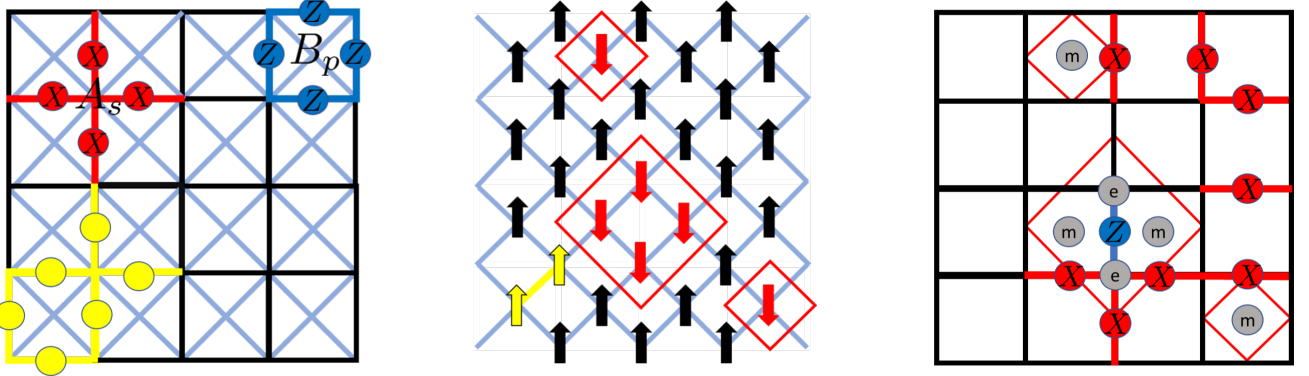


FIG. 1: (Color online.) The \mathbb{Z}_2 SPPM as an example of our duality. Left: The SPPM of Eq. (2) with star A_s , plaquette B_p , and interaction $A_s B_p$ (yellow) operators indicated. Center: The associated dual classical Ising ($q = 2$) model. The interactions $A_s B_p$ are dual to the nearest-neighbor Ising spin interactions (also highlighted in yellow). Right: An excited SPPM state created by acting with string operations on the ground-state (the dual excited Ising model state is displayed in the central panel). X and Z string excitations create m and e anyons at their endpoints.

We will analyze excitations in systems having spatially non-uniform couplings yet largely consider uniform $g_s = g_p = g$ and $J_{sp} = J$. In the square lattice realization of Eq. (2), the individual (commuting) star and plaquette operators are $A_s = X_1 X_2 X_3^\dagger X_4$ and $B_p = Z_1 Z_2 Z_3^\dagger Z_4$ with the labelling performed anti-clockwise from the upper link of the star/plaquette, and where \dagger is the adjoint. The elementary \mathbb{Z}_q “clock” and “shift” unitary operators Z_j and X_j lie on each of the N_Λ lattice links j and satisfy the Weyl algebra $X_j Z_j = e^{i2\pi/q} Z_j X_j$ [26] (generalizing the two-state ($q = 2$) Pauli algebra). The union of sites (s) and plaquette centers (p) or dual-sites forms a “diagonal lattice” highlighted in blue in Fig 1 (a.k.a. “radial lattice/graph” [27]). For $J, g > 0$, the ground-states of the SPPM and the paradigmatic \mathbb{Z}_q TC model [8, 28–30],

$$H_{\text{TC}} = - \sum_s (A_s + A_s^\dagger) - \sum_p (B_p + B_p^\dagger), \quad (3)$$

are identical with a degeneracy exponential in the genus of the lattice surface $d_{\text{TC}} = q^{2(\text{genus})}$. The SPPM and TC also share all of their excited eigenstates (with degeneracies that are integer multiples of d_{TC}). Crucially, however, the respective energies of these eigenstates will differ in both models. The first term in Eq. (2) does not appear in the TC and leads to an energy that depends on the geometrical arrangement of TC defects (anyons) where $\text{Eigenvalue}[A_s], \text{Eigenvalue}[B_p] \neq 1$.

For lattices Λ on a torus, the minimal degeneracy of each energy level of both the SPPM and the TC is associated with a pair of non-commuting symmetries (for each independent non-contractible loop C_a (or C'_a) given by (i) closed string products of Z_j operators on the lattice Λ and of (ii) X_j operators on the dual lattice Λ_d ,

$$Z_{1(2)}^q = \prod_{j \in C_{1(2)}} Z_j, \quad X_{1(2)}^q = \prod_{j \in C'_{1(2)}} X_j. \quad (4)$$

The lowest-energy excited states of the TC model are created by acting on its ground-states with products of local Z_j or local X_j operators along open strings [8]. We denote, respectively, the lattice and dual lattice strings by Z_{s_1, s_2}^q and X_{p_1, p_2}^q for strings with endpoints at sites s_1, s_2 or dual-sites p_1, p_2 . Each such string product creates an excited state of fixed energy, regardless of its length, with anyons at its endpoints. That is, there is no “string tension.” The TC anyons can drift apart an arbitrary distance without energy cost. This feature makes only the topology of the anyons (not their geometry) germane. The SPPM fundamentally differs from the TC by having additional nearest-neighbor interactions appearing in the first term of Eq. (2). These interactions produce differences in energies between nearest-neighbor and more distant anyons, introducing an effective string tension. The associated energies are identical to those of domain walls in classical clock models.

Duality between the SPPM and classical clock models. We next demonstrate that the SPPM is dual to a conventional nearest-neighbor q -state clock model. For concreteness, we analyze the SPPM on a torus. The “bond-algebra” [14, 15, 26, 31–34], i.e., the set of all independent algebraic relations amongst the individual terms appearing in the SPPM Hamiltonian is given by

$$[A_s, A_{s'}] = [A_s, B_p] = [B_p, B_{p'}] = 0, \quad (5a)$$

$$A_s^q = B_p^q = 1, \quad (5b)$$

$$(A_{s_1} B_{p_1})(A_{s_2}^\dagger B_{p_1}^\dagger)(A_{s_2} B_{p_2}) \cdots (A_{s_n} B_{p_n}) \times (A_{s_1}^\dagger B_{p_n}^\dagger) = 1, \quad (5c)$$

$$\prod_s A_s = \prod_p B_p = 1. \quad (5d)$$

Eqs. (5c) applies to the *product* of the said bilinears *along any closed loop* Γ of length $(2n)$. Eqs. (5c) are identities that follow, algebraically, from Eqs. (5a). We

have explicitly written down Eqs. (5c) in order to provide all bond-algebraic relations (including constraints amongst the individual bonds (terms) that appear in the SPPM Hamiltonian of Eq. (2)). Relations similar to Eqs. (5c) apply to products of the $(A_s B_p)$ bilinears (and their Hermitian conjugates) along an *arbitrary open contour* Γ' ; when multiplied at their two endpoints (r and m) by terms of the A_r^\dagger and/or B_m^\dagger type (or their Hermitian conjugates), such operator products along any open contour Γ' are unity. Eqs. (5a, 5b, 5c) describe the bulk theory. By contrast, Eqs. (5d) arise from periodic boundary conditions. Here, in a full lattice tiling with all stars s or plaquettes p , in the products of Eqs. (5d), each local unitary X -type operator or Z -type operator will appear twice in the product Eq. 5d.

We now turn to *classical* Landau-type nearest-neighbor q -state clock models (classical 2D Ising model for $q = 2$) in “external longitudinal fields” g_i given by the Hamiltonian

$$H_c = - \sum_{\langle i,j \rangle} J_{ij} (z_i^* z_j + z_i z_j^*) - \sum_i g_i (z_i + z_i^*), \quad (6)$$

with $z_j \in \mathbb{C}$ being q -th roots of unity. H_c is defined on the diagonal lattice of the SPPM, see Fig. 1. The diagonal lattice splinters into “even” and “odd” sub-lattices that are, respectively, associated with the sites and dual-sites of the SPPM square lattice; by comparison to Eq. (2), we set $g_i = g_s$ (even sub-lattice) and $g_i = g_p$ (odd sub-lattice) with $J_{ij} = J_{sp}$. Aside from boundary consequences (Eq. (5d)), the duality between the SPPM and the clock model is a mapping of star operators to even-site clock variables and plaquettes to odd-site clock variables and vice versa,

$$A_s \leftrightarrow z_i, \quad B_p \leftrightarrow z_j^*. \quad (7)$$

This bond-algebraic duality mapping generates the terms in the clock model from those of the SPPM, the nearest-neighbor SPPM products map to nearest-neighbor products of the classical clock model $A_s B_p \leftrightarrow z_i z_j^*$. Apart from trivial (classical) commutativity of its individual terms (similar to that of the quantum SPPM (Eq. (5a)), the bond-algebra of H_c is specified by counterparts to Eqs. (5b, 5c),

$$z_i^q = 1, \quad (8a)$$

$$\prod_{(i,j) \in \Gamma} z_i^* z_j = 1. \quad (8b)$$

Further analogous to the SPPM, the product $z_{r'} \left(\prod_{(i,j) \in \Gamma'} z_i^* z_j \right) z_{m'}^* = 1$ along *any open contour* Γ' having r' and m' as its endpoints. Similar to Eqs. (5c), these last open contour product relations and the closed contour (Γ) product equalities of Eqs. (8b) are algebraic identities. An analog of Eq. (5d) for the classical Ising ($q = 2$) case would imply that all spin

flips relative to the ferromagnetic state in the dual classical Ising model can only appear in pairs on any of the sublattices; for the general q -state clock model of Eq. (6), on each of the two sublattices, the sum of the clock spin angles must be an integer multiple of 2π . A constraint equivalent to Eq. (5d) can be realized in a clock model Hamiltonian dual by amending H_c by a pair of non-local terms [9]. Consequently, in the thermodynamic limit, the free energy density of the classical clock model is unaltered and the duality of Eq. (7) follows. Dualities between classical clock spin and SPPM systems for other boundary conditions can be found in [9].

Given the duality of Eq. (7), properties of the SPPM model can be gleaned from well-known behaviors of classical clock (and Ising) models. We list several of these. When $g = 0^+$, the global \mathbb{Z}_q symmetry of the uniform coupling classical clock model is spontaneously broken at low temperatures with *free energy barriers diverging with system size*. When $g = 0$, uniform coupling classical $q > 4$ clock models exhibit Kosterlitz-Thouless (KT) transitions (with two dual KT phase endpoints [26]); critical Ising and three-state Potts transitions appear for $q = 2, 4$ and $q = 3$ renditions respectively. H_{SPPM} realizations with random J_{sp} are dual to classical spin glass [35] models. When both J and g are uniform non-zero constants, instead of a phase transition (i.e., a non-analyticity of the free energy in the thermodynamic limit), the system may exhibit a Widom line or a weak, Kertesz [36] type, crossover known in spin models and matter coupled lattice gauge theories [37] and thus similarly do so in its SPPM dual. For random $g_{s,p}$, the SPPM maps into a classical random field model featuring numerous effects [38]. Classical ANNNI models arising for next-nearest-neighbor couplings J_{ij} [39] exhibit rich devil staircase structures. From the bond-algebraic type [14, 15, 26, 31–34] duality (7), all such behaviors of these classical clock system appear in their quantum duals.

Topological Order of the SPPM. The duality of Eq. (7) implies that any eigenstate of the clock model is also an eigenstate of the SPPM. Particularly, when $g, J > 0$, including the $g = 0^+$ limit, the ground-states of the SPPM are eigenstates of all A_s and B_p operators with an eigenvalue of 1. These eigenstates are the exact ground-states as of the TC model. By virtue of the symmetries (4), the TC model satisfies the condition of Eq. (1) and its finite temperature extension [15], and thus harbors TQO. Similar to the TC model, these (low-dimensional) generalized gauge-like symmetries [40] cannot be spontaneously broken [41–43] and endow the system with TQO [15, 16]. Since the eigenstates of the SPPM are those of the TC model, it follows that the SPPM exhibits TQO. Equivalently, any given classical clock state $\{z_i\}$ corresponds to a d_{TC} -dimensional sector of topologically degenerate SPPM eigenstates of identical $\{A_s, B_p\}$ eigenvalues that

thus cannot be told apart by local measurements [44]. The latter *topology dependent* degeneracy follows from our duality by an exponentiation $q^{E-F-V} = q^{2(\text{genus}-1)}$ of the Euler-Poincare formula to count redundant q -state operators not influencing the spectrum- the number by which the N_A local SPPM \mathbb{Z}_q operators (number of lattice edges E) exceeds the number of spins in the dual classical clock model $\{z_i\}$ (the latter being the sum of the total number of $\{B_p\}$ operators (number of lattice faces F) and of the $\{A_s\}$ operators (number of vertices V)- to the surface genus; an additional degeneracy factor of q^2 originates from the two constraints of (5d).

Excitations of the SPPM. The duality (7) allows us to find *all* SPPM excitations through their duals in the classical clock model. As we noted earlier, for $g, J > 0$, any excited state (having stars for which $\text{Eigenvalue}[A_s] \neq 1$ and/or plaquettes $\text{Eigenvalue}[B_p] \neq 1$) is also an excitation of the \mathbb{Z}_q TC model of Eq. (3). Notably, different from other systems exhibiting TC ground-states [45], the identical spectra of the SPPM and classical clock model are trivially quantized (given by sums of integer multiples of the coupling constants times cosines of the q allowed discrete clock angles). Thus, in particular, the SPPM is gapped allowing for stable anyon excitations. An anyon in the \mathbb{Z}_q TC model, $\epsilon^{n,\ell}$ with $0 \leq n, \ell \leq (q-1)$, is a composite of n minimal “electric” charges e on the lattice sites (here, $e = \epsilon^{1,0}$) and ℓ basic “magnetic” charges m (with $m = \epsilon^{0,1}$) associated with dual-sites. The energy of different TC eigenstates depends only on anyon type and number. By contrast, in the SPPM, even the energies of the lowest-energy excitations may depend on the geometry, e.g., whether the anyons are nearest-neighbors.

The statistics in general lowest-energy states need not correspond to ideal braiding of individual fundamental charges. Indeed, in general applications of the duality of Eq. (7), *lowest-energy* (gapped) excited states of the classical spin system may involve *non-compact* configurations such as the lowest-lying excited states of spin-glass [35, 46], ANNNI [39], and other models. When the lowest-energy excitations of these classical systems are spatially non-compact, the duality (7) implies that the corresponding lowest-energy excitations of the quantum system are, similarly, not lone point excitations but may, instead, be rich composites of many point charges. A simple example is the SPPM (2) on a torus with $J_{sp} = J > 0$ and vanishing fields $g_s = g_p = 0$ at all sites s and plaquettes p except for $s = 0$, where $8J > g_{s=0} > 0$. Here, the classical system has the ferromagnetic ground-state $z_i = 1$ corresponding to conventional TC TQO on the quantum side of the duality (7) where $\forall s, p : \text{Eigenvalue}[A_s] = \text{Eigenvalue}[B_p] = 1$ with, on the torus, a $d_{TC} = q^2$ -dimensional ground-state manifold satisfying Eq. (1). The lowest-energy excited states correspond to different uniform classical clock model ferromagnetic states (and, thus, uniform dual A_s and B_p eigenvalues) associated with a global rotation by $2\pi/q$ [47]. When

$q = 2$, the d_{TC} degenerate lowest-energy eigenstates of the SPPM are the highest-energy eigenstates of the TC ($\forall s, p : \text{Eigenvalue}[A_s] = \text{Eigenvalue}[B_p] = -1$). These eigenstates correspond to *maximally dense alternating e and m charges covering the entire lattice* (albeit being non-local in real-space, these lowest-energy excitation are local in k -space). Since the anyons are everywhere in space, realizing pristine long-distance operations involving only individual anyons may be physically challenging. Formally, anyon operations may be carried out in general spaces.

Conclusions. Various models displaying TQO (satisfying the ground-state indistinguishability condition of Eq. (1)) exhibit excitations that lie beyond conventional TQFT descriptions. To demonstrate this, we introduced models containing distance dependent interactions (emulating perturbations) between anyons of known parent TC models. Such additional anyon interactions are expected in experimental realizations. To analyze these models, we demonstrated that particular TQO \mathbb{Z}_q systems are dual to classical clock type models. Unlike thermally fragile [43] TC and other topological models [23] that map onto one-dimensional systems, our models are identical to conventional high-dimensional Landau-type theories. The lowest-energy excited states of our systems *do not* necessarily correspond to single localized anyons for which conventional TQFT considerations apply. Instead, in the thermodynamic limit, these *lowest-energy excitations* may correspond to an *infinite size dense lattice of anyons*. The *divergent* number of space-filling anyons in such states lies beyond known TQFT applications. There are illuminating connections between quantum error correcting (surface) codes and TQO as established by writing Hamiltonians in terms of stabilizer group generators [48], and encoding code words in ground-states. Our models include elements of the stabilizer group (e.g., the products $\{(A_s B_p)\}$), augmenting independent $\{(A_s), \{B_p\}\}$ generators. This inclusion leads to new physics. Indeed, as we emphasized, the $J = 0$ SPPM (i.e., \mathbb{Z}_q TC model) is dual to decoupled one-dimensional chains [15, 16, 43] while for $J \neq 0$ (when products $\{(A_s B_p)\}$ appear in H_{SPPM}), no such dimensional reduction results; the resulting dual high-dimensional classical systems may display large free energy barriers rendering them more immune to thermal fluctuations. In [9], we expound on similar generalizations of string-net and other (including higher-dimensional) models and their various features. Our models realize quantum codes not explored to date.

Acknowledgments. We are indebted to conversations with Erez Berg, Jean-Noel Fuchs, Alexander Seidel, Steve Simon, Ruben Verresen, and Julien Vidal. ZN is grateful to the Leverhulme-Peierls senior researcher Professorship at Oxford supported by a Leverhulme Trust International Professorship grant [number LIP-2020-014]. This research was undertaken thanks in part to funding

from the Canada First Research Excellence Fund.

* corresponding author: zohar@wustl.edu

- [1] Edward Witten. Topological Quantum Field Theory. *Commun. Math. Phys.*, 117:353, 1988. doi: 10.1007/BF01223371.
- [2] Michael Atiyah. Topological quantum field theories. *Publications mathématiques de l'IHÉS*, 68(1):175–186, 1988. doi:10.1007/bf02698547.
- [3] Edward Witten. Quantum field theory and the Jones polynomial. *Communications in Mathematical Physics*, 121(3):351 – 399, 1989.
- [4] Jacob Lurie. On the classification of topological field theories, 2009. URL <https://arxiv.org/abs/0905.0465>.
- [5] Sergei Gukov and Anton Kapustin. Topological quantum field theory, nonlocal operators, and gapped phases of gauge theories, 2013. URL <https://arxiv.org/abs/1307.4793>.
- [6] Chi-Ming Chang, Ying-Hsuan Lin, Shu-Heng Shao, Yifan Wang, and Xi Yin. Topological Defect Lines and Renormalization Group Flows in Two Dimensions. *JHEP*, 01: 026, 2019. doi:10.1007/JHEP01(2019)026.
- [7] Steve Simon. *Topological Quantum*. Oxford University Press, 2023.
- [8] A.Yu. Kitaev. Fault-tolerant quantum computation by anyons. *Annals of Physics*, 303(1):2–30, 2003. doi: 10.1016/s0003-4916(02)00018-0.
- [9] Supplemental material.
- [10] Chien-Hung Lin, Michael Levin, and Fiona J. Burnell. Generalized string-net models: A thorough exposition. *Physical Review B*, 103(19), may 2021. doi: 10.1103/physrevb.103.195155. URL <https://doi.org/10.1103%2Fphysrevb.103.195155>.
- [11] Michael A. Levin and Xiao-Gang Wen. String-net condensation: a physical mechanism for topological phases. *Physical Review B*, 71(4), jan 2005. doi: 10.1103/physrevb.71.045110. URL <https://doi.org/10.1103%2Fphysrevb.71.045110>.
- [12] Oliver Buerschaper and Miguel Aguado. Mapping kitaev’s quantum double lattice models to levin and wen’s string-net models. *Physical Review B*, 80(15), oct 2009. doi:10.1103/physrevb.80.155136. URL <https://doi.org/10.1103%2Fphysrevb.80.155136>.
- [13] Jiannis K. Pachos. *Introduction to topological Quantum Computation*. Cambridge University Press, 2012.
- [14] Emilio Cobanera, Gerardo Ortiz, and Zohar Nussinov. The bond-algebraic approach to dualities. *Advances in Physics*, 60(5):679–798, 2011.
- [15] Zohar Nussinov and Gerardo Ortiz. A symmetry principle for topological quantum order. *Annals of Physics*, 324(5):977–1057, 2009. doi:10.1016/j.aop.2008.11.002.
- [16] Zohar Nussinov and Gerardo Ortiz. Sufficient symmetry conditions for topological quantum order. *Proceedings of the National Academy of Sciences of the United States of America*, 106:16944–16949, 2009.
- [17] Andrej Mesaros and Ying Ran. Classification of symmetry enriched topological phases with exactly solvable models. *Physical Review B*, 87(15), apr 2013. doi: 10.1103/physrevb.87.155115. URL <https://doi.org/10.1103%2Fphysrevb.87.155115>.
- [18] Jeongwan Haah. Local stabilizer codes in three dimensions without string logical operators. *Physical Review A*, 83(4), April 2011. ISSN 1050-2947, 1094-1622. doi: 10.1103/PhysRevA.83.042330. URL <https://link.aps.org/doi/10.1103/PhysRevA.83.042330>.
- [19] Beni Yoshida. Exotic topological order in fractal spin liquids. *Physical Review B*, 88(12), sep 2013. doi: 10.1103/physrevb.88.125122. URL <https://doi.org/10.1103%2Fphysrevb.88.125122>.
- [20] Sagar Vijay, Jeongwan Haah, and Liang Fu. A new kind of topological quantum order: A dimensional hierarchy of quasiparticles built from stationary excitations. *Physical Review B*, 92:235136, 2015.
- [21] Kevin Slagle and Yong Baek Kim. X-cube model on generic lattices: Fracton phases and geometric order. *Physical Review B*, 97(16), apr 2018. doi: 10.1103/physrevb.97.165106. URL <https://doi.org/10.1103%2Fphysrevb.97.165106>.
- [22] Rahul M Nandkishore and Michael Hermele. Fractons. *Annual Review of Condensed Matter Physics*, page 295, 2019.
- [23] Zack Weinstein, Gerardo Ortiz, and Zohar Nussinov. Universality classes of stabilizer code hamiltonians. *Phys. Rev. Lett.*, 123:230503, Dec 2019. doi: 10.1103/PhysRevLett.123.230503. URL <https://link.aps.org/doi/10.1103/PhysRevLett.123.230503>.
- [24] Michael Pretko, Xie Chen, and Yizhi You. Fracton phases of matter. *International Journal of Modern Physics A*, 35:2030003, 2020.
- [25] Z. Nussinov and G. Ortiz. A theorem on extensive spectral degeneracy for systems with rigid higher symmetries in general dimensions. *Physical Review B*, 107:045109, 2023.
- [26] G. Ortiz, E. Cobanera, and Z. Nussinov. Dualities and the phase diagram of the p-clock model. *Nuclear Physics B*, 854(3):780–814, 2012. ISSN 0550-3213. doi: <https://doi.org/10.1016/j.nuclphysb.2011.09.012>. URL <https://www.sciencedirect.com/science/article/pii/S0550321311005219>.
- [27] Lowell Abrams and Daniel Shlafly. A basic structure for grids in surfaces, 2019. URL <https://arxiv.org/abs/1901.03682>.
- [28] Marc Daniel Schulz, Sébastien Dusuel, Román Orús, Julien Vidal, and Kai Phillip Schmidt. Breakdown of a perturbed topological phase. *New Journal of Physics*, 14(2):025005, feb 2012. doi:10.1088/1367-2630/14/2/025005. URL <https://doi.org/10.1088%2F1367-2630%2F14%2F2%2F025005>.
- [29] Daniel Gottesman. Stabilizer codes and quantum error correction, 1997. URL <https://arxiv.org/abs/quant-ph/9705052>.
- [30] M. F. Araujo de Resende. A pedagogical overview on 2d and 3d toric codes and the origin of their topological orders. *Reviews in Mathematical Physics*, 32(02):2030002, aug 2019. doi:10.1142/s0129055x20300022. URL <https://doi.org/10.1142%2Fs0129055x20300022>.
- [31] Z. Nussinov and G. Ortiz. Bond algebras and exact solvability of hamiltonians: Spin $s=1/2$ multilayer systems and other curiosities. *Physical Review B*, 79:21444, 2009.
- [32] E. Cobanera, G. Ortiz, and Z. Nussinov. Unified approach to classical and quantum dualities. *Physical Review Letters*, 104:020402, 2010.
- [33] Zohar Nussinov, Gerardo Ortiz, and Emilio Cobanera. Arbitrary dimensional majorana dualities and network

architectures for topological matter. *Physical Review B*, 86:085415, 2012.

[34] Z. Nussinov and G. Ortiz. Orbital order driven quantum criticality. *Europhysics Letters*, 84, 2008.

[35] Marc Mezard, Giorgio Parisi, and Miguel Angel Virasoro. *Spin glass theory and beyond*. Singapore: World Scientific, 1987. ISBN 978-9971-5-0115-0.

[36] J. Kertesz. Existence of weak singularities when going around the liquid-gas critical point. *Physica A*, 161:58, 1989.

[37] Z. Nussinov. Derivation of the fradkin-shenker result from duality: Links to spin systems in external magnetic fields and percolation crossovers. *Physical Review D*, 72: 54509, 2005.

[38] S. Rychkov. *Lectures on the Random Field Ising Model, From Parisi-Sourlas Supersymmetry to Dimensional Reduction*. Springer Briefs in Physics, 2023.

[39] W. Selke. The annni model- theoretical analysis and experimental application. *Physics Reports*, 170:213, 1988.

[40] John McGreevy. Generalized symmetries in condensed matter. *Annual Review of Condensed Matter Physics*, 14:57, 2022.

[41] Cristian D. Batista and Zohar Nussinov. Generalized elitzur’s theorem and dimensional reductions. *Physical Review B*, 72:045137, 2005.

[42] Z. Nussinov, G. Ortiz, and E. Cobanera. Effective and exact holographies from symmetries and dualities in quantum systems. *Annals of Physics*, 327:2491, 2012.

[43] Zohar Nussinov and Gerardo Ortiz. Autocorrelations and thermal fragility of anyonic loops in topologically quantum ordered systems. *Physical Review B*, 77(6), feb 2008. doi:10.1103/physrevb.77.064302. URL <https://doi.org/10.1103%2Fphysrevb.77.064302>.

[44] Note1. Operators having different expectation values involve the non-local symmetries (4).

[45] Carlos Fernandez-Gonzalez, Norbert Schuch, Michael M. Wolf, Ignacio Cirac, and David Perez-Garcia. Gapless hamiltonians for the toric code using the peps formalism. *Phys. Rev. Lett.*, 109:260401, 2012.

[46] S. Mutian, G. Ortiz, Y-Y. Liu, M. Weigel, and Z. Nussinov. Universal fragility of spin-glass ground-states under single bond changes. *arXiv*, 2023. URL <https://arxiv.org/abs/2305.10376>.

[47] Note2. Relative to the ground-state, the energy penalty of global $(2\pi/q)$ rotations stems from the difference between the resulting $A_{s=0}$ eigenvalue (associated with an ensuing phase factor of $(2\pi/q)$) with that favored by the external longitudinal field $g_{s=0}$ (i.e., an $A_{s=0}$ eigenvalue of unity suffering no such rotation). When $g_{s=0} > 8J > 0$, the latter penalty will exceed that of states having a $(2\pi/q)$ phase factor of only two eigenvalues of either the star or the plaquette operators (or of two classical clock spins lying on the same sublattice in the dual model) with all other A_s and B_p eigenvalues (respectively, classical clock spin variables z_i) being $(+1)$. The above factor of eight in $8J$ arises from the product of two (the minimal number of disjoint $s \neq 0$ star or plaquette operator eigenvalues (classical clock spin variables) that may differ from unity given constraint (5d)) and four (the length of the smallest square lattice domain wall around each of these rotated $s \neq 0$ star or plaquette eigenvalues (respectively, classical clock spins)).

[48] A Ashikhmin and E. Knill. Nonbinary quantum stabilizer codes. *IEEE Trans. Inf. Theory*, 47:3065, 2001.

[49] Mohammad-Sadegh Vaezi, Gerardo Ortiz, and Zohar Nussinov. Robust topological degeneracy of classical theories. *Physical Review B*, 93(20), may 2016. doi:10.1103/physrevb.93.205112. URL <https://doi.org/10.1103%2Fphysrevb.93.205112>.

[50] Xiao-Gang Wen. Topological order: From long-range entangled quantum matter to a unified origin of light and electrons. *ISRN Condensed Matter Physics*, 2013: 1–20, mar 2013. doi:10.1155/2013/198710. URL <https://doi.org/10.1155%2F2013%2F198710>.

[51] B J Hiley and G S Joyce. The ising model with long-range interactions. *Proceedings of the Physical Society*, 85(3):493–507, 1965. doi:10.1088/0370-1328/85/3/310.

[52] Anna Kómár and Olivier Landon-Cardinal. Anyons are not energy eigenspaces of quantum double hamiltonians. *Phys. Rev. B*, 96:195150, Nov 2017. doi:10.1103/PhysRevB.96.195150. URL <https://link.aps.org/doi/10.1103/PhysRevB.96.195150>.

[53] Julien Vidal. Partition function of the levin-wen model. *Physical Review B*, 105(4), jan 2022. doi:10.1103/physrevb.105.104110. URL <https://doi.org/10.1103%2Fphysrevb.105.104110>.

[54] A. Ritz-Zwilling, Jean-Noel Fuchs, Steven H. Simon, and Julien Vidal. Topological and nontopological degeneracies in generalized string-net models, 2023. URL <https://arxiv.org/abs/2309.00343>.

[55] Liang Kong, Yin Tian, and Zhi-Hao Zhang. Defects in the 3-dimensional toric code model form a braided fusion 2-category. *Journal of High Energy Physics*, 2020(12), dec 2020. doi:10.1007/jhep12(2020)078. URL <https://doi.org/10.1007%2Fjhep12%282020%29078>.

**SUPPLEMENTAL MATERIAL:
TOPOLOGICAL ORDERS BEYOND TOPOLOGICAL QUANTUM FIELD THEORIES**

P. Vojta, G. Ortiz, and Zohar Nussinov*

In what follows, we expand on various aspects.

**FURTHER DETAILS OF DUALITY MAPPINGS
OF THE SPPM TO CLASSICAL CLOCK MODELS**

**Mapping an SPPM on an Open Surface to a
Classical Clock Model**

Here, we consider the duality mapping between an “open boundary condition” planar SPPM to a square lattice classical clock model. In this mapping, clock spins of the classical model are duals of the star or plaquette terms of the SPPM. On the boundary of the planar SPPM system, we define star and plaquette operators to include only those links that still lie in the lattice. The products $\prod_s A_s$ and $\prod_p B_p$ will now act on boundaries and are unconstrained (do not satisfy Eq. (5d)). The result is a dual classical clock model on the same lattice with a number of clock model spins that is equal to that of the number of bonds in the quantum system (Eq. (7)). If the number of independent bonds or generators, i.e., the sum of the number of star and plaquette terms, $(N_s + N_p)$ is smaller than the number of links, there will be an additional degeneracy factor of $q^{(N - N_s - N_p)}$. For simple boundaries, this will result in a global “holographic degeneracy” [49]- a degeneracy scaling exponentially in the system boundary length.

**Mapping an SPPM on a Torus to a Classical Clock
Model**

We now examine the duality between the SPPM on a torus (periodic boundary conditions) and a classical clock model. The incorporation of the periodic boundary condition constraint of Eq.(5d) can be achieved by amending the classical clock model Hamiltonian H_c of Eq. (6) by a finite number of bounded non-local terms (that sum to δH_c). Towards this end, for any particular even (\tilde{s}) and odd (\tilde{p}) sublattice sites the two operators amending the classical clock model Hamiltonian H_c of Eq. by a finite number of bounded non-local terms (δH_c). Towards this end, for any particular even (\tilde{s}) and odd (\tilde{p}) sublattice sites the two operators

$$\mathcal{W}_{\tilde{s}} \equiv \prod_{j \text{ even}, j \neq \tilde{s}} z_j, \quad \mathcal{W}_{\tilde{p}}^* \equiv \prod_{k \text{ odd}, k \neq \tilde{p}} z_k^*. \quad (9)$$

With these, we perform the mapping of Eq. (7) with the modification that for sites \tilde{s} and \tilde{p} we instead replace

$$A_{\tilde{s}} \leftrightarrow \prod_{j \text{ even}, j \neq \tilde{s}} z_j = \mathcal{W}_{\tilde{s}}, \quad B_{\tilde{p}} \leftrightarrow \prod_{k \text{ odd}, k \neq \tilde{p}} z_k^* = \mathcal{W}_{\tilde{p}}^*. \quad (10)$$

With the mapping of Eq. (10), the product of all clock spin variables in the respective even and odd partitions will satisfy the global SPPM constraint of Eq. (5d). Thus, out of the N classical clock model spins, one pair of spins become redundant (fixed by the products of spins on other sites as on the righthand side of Eq. (10)) and will not impact the energy of the N spin model. That is, by comparison to the N site classical clock model, there is an additional uniform global degeneracy factor of q^2 of each level (i.e., a factor of q for each of the two classical spins at sites \tilde{s} and \tilde{p} that will no longer impact the system energy once the substitution of Eq. (10) is implemented into the system Hamiltonian). This degeneracy can also be read off from the two \mathbb{Z}_q symmetries of the system (Eq. (4)) highlighted in Fig. 2. A detailed list of operators in the two models connected by this particular duality is given in Table I.

Performing the duality of Eqs. (7, 10) to the SPPM Hamiltonian of Eq. (2) on a system with periodic boundary conditions (where Eq. (5d) applies) leads to a classical spin model with the said Hamiltonian of $(H_c + \delta H_c)$. The precise form of δH_c depends on whether \tilde{s} and \tilde{p} are nearest-neighbors. When, e.g., \tilde{s} and \tilde{p} are well separated,

$$\begin{aligned} \delta H_c = & -J \sum_{\langle j \tilde{p} \rangle} \mathcal{W}_{\tilde{p}}^* z_j + \mathcal{W}_{\tilde{p}} z_j^* - g(\mathcal{W}_{\tilde{p}} + \mathcal{W}_{\tilde{p}}^*) \\ & - J \sum_{\langle k \tilde{s} \rangle} \mathcal{W}_{\tilde{s}}^* z_k + \mathcal{W}_{\tilde{s}} z_k^* - g(\mathcal{W}_{\tilde{s}} + \mathcal{W}_{\tilde{s}}^*) \\ & + J \sum_{\langle i \tilde{p} \rangle} z_{\tilde{p}}^* z_j + z_{\tilde{p}} z_j^* + g(z_{\tilde{p}} + z_{\tilde{p}}^*) \\ & + J \sum_{\langle k \tilde{s} \rangle} z_{\tilde{s}}^* z_k + z_{\tilde{s}} z_k^* + g(z_{\tilde{s}} + z_{\tilde{s}}^*). \end{aligned} \quad (11)$$

This Hamiltonian is a function of $(N - 2)$ independent spins once Eq. (10) is implemented. Thus, on the 4-fold coordinated square lattice, $|\delta H_c| \leq (32J + 8g)$ (here the prefactor of 32 originates from the product of 8 (number of relevant terms) \times 4 (lattice coordination number)). An individual clock spin (at an arbitrary site j) can be written as $z_j = e^{2i\pi k_j/q}$, $k_j = 0, 1, \dots, q - 1$. With this substitution, the clock model Hamiltonian of Eq. (6) then reads

$$H_c = -2J \sum_{\langle i, j \rangle} \cos\left(\frac{2\pi(k_i - k_j)}{q}\right) - 2g \sum_j \cos\left(\frac{2\pi k_j}{q}\right). \quad (12)$$

In what follows, we first briefly discuss the $J = 0$ case (the \mathbb{Z}_q TC model) and then turn to the SPPM ($J \neq 0$).

For $J = 0$, we may employ a trivial generalization of the duality mapping of [15] so that the \mathbb{Z}_q TC model ($J = 0$) is dual to a pair of uncoupled periodic \mathbb{Z}_q clock model spin chains. In this $J = 0$ limit, denoting the clock spin variables in the first periodic chain by $z^{(1)}$ and those in the second chain by $z^{(2)}$ gives the dual classical clock model Hamiltonian

$$H_c^{\text{chains}} = -g \sum_{i=1}^N (z_i^{(1)*} z_{i+1}^{(1)} + z_j^{(1)} z_{j+1}^{(1)*}) - g \sum_{j=1}^N (z_j^{(2)*} z_{j+1}^{(2)} + z_j^{(2)} z_{j+1}^{(2)*}). \quad (13)$$

Here, the corresponding partition functions are quite simple to calculate via the transfer matrices of the model. The discrete clock rotation invariant transfer matrix may be diagonalized by a discrete Fourier transform. For the single chain, the partition function reads

$$\mathcal{Z}_c^{\text{chain}} = \sum_{\tilde{n}=1}^q \left(\sum_{n=1}^q \exp \left(2g \cos \left(\frac{2\pi n}{q} \right) + i \frac{2\pi n \tilde{n}}{q} \right) \right)^N. \quad (14)$$

In the $N \rightarrow \infty$ limit, the non-oscillatory $\tilde{n} = 0$ term dominates over all other Fourier components. in Eq. (14),

$$\mathcal{Z}_c^{\text{chain}} \approx \left(\sum_{n=1}^q \left(\exp \left(2g \cos \left(\frac{2\pi n}{q} \right) \right) \right)^N. \quad (15)$$

Thus in the thermodynamic limit, the partition function of the $J = 0$ SPPM model (\mathbb{Z}_q TC model) which is the product of partition functions of two identical chains, $\mathcal{Z}_{c,1}^{\text{chain}} \times \mathcal{Z}_{c,2}^{\text{chain}}$, is given by the square of Eq. (15).

We now return to the general case of arbitrary J (the SPPM). Here, the duality implies that the free energy density of the SPPM whose classical dual is given by $(H_c + \delta H_c)$ is identical to that of the conventional clock model of H_c . As we discussed above, taking into account the constraints of Eq. (10), there is a global degeneracy of q^2 of each level. The $q \rightarrow \infty$ limit yields a duality to a classical XY model.

MAPPING CLASSICAL CLOCK MODELS TO SPPM SYSTEMS

We now discuss the “inverse” of the above mapping and illustrate how to map a conventional classical clock model on a torus onto a modified SPPM type system. For periodic boundary conditions, the SPPM satisfies the constraint of Eq. (5d). Previously, we discussed the mapping from the SPPM to the clock model while preserving this constraint. Now we examine a map from the classical spin model to the SPPM which preserves

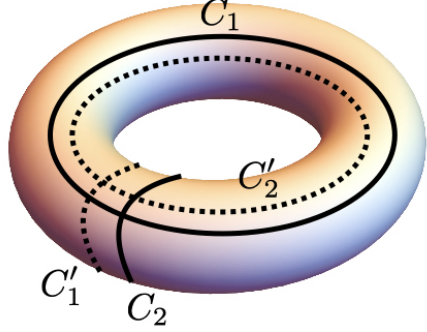


FIG. 2: The $d = 1$ topologically distinct loops of the \mathbb{Z}_q TC (associated with the symmetry operators of Eq. (4)). The $Z_{1(2)}^q$ symmetries (that constitute logical operators of the TC) are given by products of Pauli matrices on the solid lines $C_{1,2}$ that pass through the lattice sites. The dashed lines $C'_{1,2}$ inhabit the dual lattice and host the logical operators $X_{1(2)}^q$.

SPPM	Clock Model
A_s	z_i (even)
B_p	z_j^* (odd)
$\prod_s A_s$	$\mathbb{1}$
$\prod_p B_p$	$\mathbb{1}$
$X_{1(2)}^q$ or $Z_{1(2)}^q$	$\mathbb{1}$
Z_{s_1, s_2}^q	$x_{s_1} x_{s_2}$
X_{p_1, p_2}^q	$x_{p_1} x_{p_2}$
$A_{\tilde{s}}$	$\prod_j \text{even, } j \neq \tilde{s} z_j^*$
$B_{\tilde{p}}$	$\prod_k \text{odd, } k \neq \tilde{p} z_k^*$
$X_{\tilde{p}, s(x_i)}^q$ or $Z_{\tilde{s}, p(x_i)}^q$	x_i
U_{sp}	$\prod_i x_i$

TABLE I: Correspondences between the operators in the SPPM of Eq. (2) and clock model operators of Eq. (6).

looser constraints. We will see that each link-local operation X or Z corresponds to flipping a pair of diagonally neighboring clock spins. This enforces the dual constraint of pairwise flipping spins and preserving the spin parity number. However this constraint is not valid in the clock model, where a single clock spin can always be rotated. So conventional clock models with periodic boundary conditions will not map into SPPMs with periodic boundary conditions unless we include additional degrees of freedom. We next consider various types of periodic clock models and their SPPM duals.

“Even-Sized” Square Lattices

We first consider a classical clock model on a square lattice (of size $L_1 \times L_2$) on a torus and map it into an SPPM-like model on a lattice that is endowed with periodic boundary conditions. When both L_1 and L_2

are even, the classical spin model vertex to SPPM star/plaquette operator mapping (an inverse of Eq. (7)) may be applied everywhere relating the original square lattice on which the classical clock model is defined to the 45° rotated square lattice on which an SPPM type model is defined (see Fig. 1). This mapping will result in $\prod_s A_s$ and $\prod_p B_p$ being unconstrained, unlike Eq. 5d. To make an analog of these products unconstrained in the SPPM like model, we introduce two independent \mathbb{Z}_q operators Ω_1 and Ω_2 . With these, we replace the individual star and plaquette operators A_s and B_p in Eq. (2) by, respectively,

$$\bar{A}_s \equiv \Omega_1 A_s, \quad \bar{B}_p \equiv \Omega_2 B_p. \quad (16)$$

The operators Ω_1 and Ω_2 correspond to two fully decoupled \mathbb{Z}_q redundant gauge-like degrees of freedom leading to a q^2 -fold degeneracy.

“Odd-Sized” Square Lattices

We now turn to duality mappings from a classical clock model on a torus to an SPPM type system for square lattices when, at least, one of the sides L_1 or L_2 is odd. Here, the constructs of Eq. (16) may still be applied, allowing for the desired lack of constraints 5c. In this case, the geometrical implementation of Eq. (10) (Fig. (1)) will not be consistent at the boundaries of the square lattice on which the classical clock model is defined. We can resolve this by constructing boundary operators \mathcal{B}_i that will obey constraints equivalent to those in Eq. 5a-5d. Towards that end, we introduce new operator products $\mathcal{B}_{+/-}$ that act on both sides of the “boundary” as shown in Fig. 3. We further introduce a corner operator \mathcal{B}_c if both L_1 and L_2 are odd. These boundary terms are now further included in the amended Hamiltonian of Eq. (2) with the replacement of star and plaquette terms following Eq. (16). Neighboring \mathcal{B}_i overlap by one link and all \mathcal{B}_i map individually into the clocks to which the disconnect has been associated. These disconnects generally replace the constraint of Eq. (5d) by the looser condition of $\prod_s A_s \prod_p B_p \prod_{\forall \mathcal{B}} \mathcal{B} = 1$. However, with modifications of Eq. 16, the respective global products are unconstrained.

DUAL OPERATORS TO SINGLE CLOCK ROTATION AND GLOBAL SYMMETRIES

We now further consider the operators connected by dualities between clock models and SPPMs. We seek operators with isomorphic actions on the respective bond-algebra. Consider an on-site clock rotation at site k in the clock model

$$x_k : z_j \leftrightarrow \begin{cases} e^{i2\pi/q} z_j & \text{if } j = k \\ z_j & \text{otherwise} \end{cases}. \quad (17)$$

If $z_j \leftrightarrow A_s$ under the inverse duality map, then the respective transformation for the star operators reads

$$A_l \leftrightarrow \begin{cases} e^{i2\pi/q} A_l & \text{if } j = k \\ A_l & \text{otherwise} \end{cases}. \quad (18)$$

The transformation for the plaquette operators is analogous. Certain operators with this action exist but depend heavily on boundary conditions. For the periodic SPPM discussed in the main text, with the modifications of Eq. 11, we notice that x_k also rotates one of the respective \mathcal{W} ’s. That is, the x_k operators act like (and are in fact dual to) $Z_{\tilde{s},s}^q$ and $X_{\tilde{p},p}^q$.

$$Z_{\tilde{s},s}^q = \prod_{j \in C_{\tilde{s},s}} Z_j, \quad X_{\tilde{p},p}^q = \prod_{j \in C'_{\tilde{p},p}} X_j. \quad (19)$$

Here, $C_{\tilde{s},s}$ is a contour in the lattice with endpoints at s and \tilde{s} while $C'_{\tilde{p},p}$ is similarly placed in the dual-lattice with endpoints at p and \tilde{p} .

Given a conventional classical clock model with periodic boundary conditions, consider a duality to an SPPM with the modifications of Eq. (16). We next construct the dual string products

$$\bar{Z}_{\tilde{s},s}^q = x_{\Omega_1}^{-1} \prod_{j \in C_{\tilde{s},s}} Z_j, \quad \bar{X}_{\tilde{p},p}^q = x_{\Omega_2}^{-1} \prod_{j \in C'_{\tilde{p},p}} X_j. \quad (20)$$

Here, we amended the string products with counter-rotating operators on Ω so as to leave the operators \bar{A}_s and \bar{B}_p of Eq. (16) unchanged. For an SPPM on the infinite planar lattice or embedded on a manifold with a boundary, x_k is dual to a product along a string-like contour with this contour either diverging to infinity or terminating on the boundary, respectively.

The $J, g > 0$ SPPM has a ground-state subspace identical to that of the TC ground-state subspace, V_{TC} . We know the classical clock model at $g = 0$ has a global symmetry \mathcal{U}_{clock} . Removing g -terms from the SPPM also introduces a global symmetry into the system. The $J > 0, g = 0$ SPPM ground-states are specified by the condition $A_s |\psi\rangle = B_p^\dagger |\psi\rangle = e^{i2n\pi/q} |\psi\rangle$, $n = 0, 1, 2, \dots, q - 1$. The respective $n = 0$ subspace is then that of the TC model, V_{TC} . The global symmetry group generated by an operator \mathcal{U}_{sp} , detailed below, then connects the q subspaces which correspond respectively to the q ground-states of the dual $g = 0$ clock model.

Specifically, the global rotational symmetry of a conventional clock model is

$$\mathcal{U}_{clock} = \prod_j x_j. \quad (21)$$

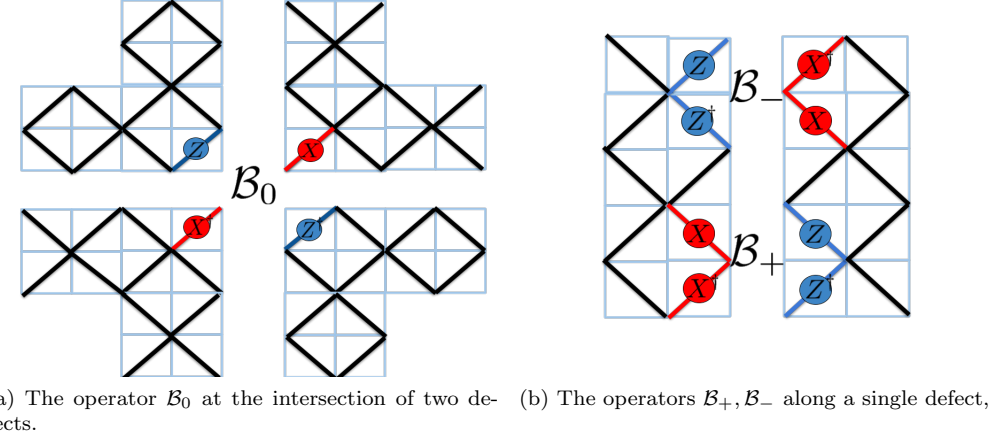


FIG. 3: (Color online.) Stitching operators $\mathcal{B}_0, \mathcal{B}_+, \mathcal{B}_-$ obey the same general bond-algebraic constraints. They can be used to pass strings/anyons across the defects. The SPPM lattice is in black and the corresponding \mathbb{Z}_2 clock lattice is in light blue.

The dual symmetry is then generally the appropriate aforementioned product of strings, forming the global symmetry of the SPPM. For the periodic SPPM discussed in the main text (with the modifications of Eq. 10 in the dual clock model at \tilde{p} and \tilde{s}) the global symmetry is simply

$$\mathcal{U}_{sp} = \left(\prod_p X_{\tilde{p},p}^q \right) \left(\prod_s Z_{\tilde{s},s}^q \right). \quad (22)$$

An alternative view of topological order centers on long-range entanglement [50]. Here, \mathcal{U}_{sp} is a tensor product, leaving the known long-range entanglement features of V_{TC} unchanged. The two factors of \mathcal{U}_{sp} also have natural interpretations in the $q = 2$ (i.e., Ising) model. They connect the ferromagnetic ground-states to the ground-states of its antiferromagnetic phase. The global X -string product in Eq. (22), which generates m -type anyons on all plaquettes, is dual to an operator which globally rotates all classical clock model spins on sites of the odd sublattice.

In the TC, an application of \mathcal{U}_{sp} on the ground-state generates anyons uniformly at every site and dual-site (i.e., plaquette center) of the lattice. The SPPM nearest neighbor coupling (J type) terms do not distinguish between the TC vacuum $|k, 0\rangle$ and anyon populated states $|k, n\rangle = \mathcal{U}^n |k, 0\rangle$ where $k = 1, 2, \dots, q^{2(\text{genus})}$ and $n = 0, 1, \dots, q - 1$. For these states, $A_s |k, n\rangle = e^{i2n\pi/q} |k, n\rangle$ and $B_p |k, n\rangle = e^{-i2n\pi/q} |k, n\rangle$. With the $\epsilon^{n,\ell}$ excitation taxonomy of the main text, the action of \mathcal{U}_{sp} ,

$$\mathcal{U}_{sp} : \epsilon^{n,\ell} \mapsto \epsilon^{n+1,\ell+1}. \quad (23)$$

Thus,

$$\mathcal{U}_{sp}(\epsilon^{n,\ell} \times \epsilon^{u,v}) = \mathcal{U}_{sp}(\epsilon^{n+u,\ell+v}) = \epsilon^{n+u+1,\ell+v+1}, \quad (24)$$

while

$$\begin{aligned} \mathcal{U}_{sp}(\epsilon^{n,\ell}) \times \mathcal{U}_{sp}(\epsilon^{u,v}) &= \epsilon^{n+u+2,\ell+v+2} \\ &\neq \mathcal{U}_{sp}(\epsilon^{n,\ell} \times \epsilon^{u,v}). \end{aligned} \quad (25)$$

In other words, the TC excitation algebra does not remain invariant under a transformation by \mathcal{U}_{sp} . When $g = 0$, both the (i) vacuum and (ii) the maximally possible dense anyon state are ground-states of the SPPM. New, but related, descriptions are required to accurately capture the behavior of the excitations which in this model are merely the domain walls between differing regions locally forming a ground-state.

SPPM VARIANTS AND THEIR EXCITATIONS

Long-range models

Our construct is not limited to short-range interactions. Consider a long-range Ising model [51] governed by the Hamiltonian ($J > 0$),

$$H_{\text{LRI}} = - \sum_{i < j} \frac{J}{|r_i - r_j|^\zeta} \sigma_i \sigma_j - g_i \sum_i \sigma_i, \quad (26)$$

with $\sigma_i = \pm 1$. In order for a ferromagnetic ground-state in D dimensions to have a well defined finite energy density in the thermodynamic limit, the exponent $\zeta > D$. Repeating our earlier steps (in particular, those relating to the mapping of Eq. (7)) yields a quantum dual given

by

$$H_{\text{LRSP}} = - \sum_{s,p} \frac{J}{|r_s - r_p|^\zeta} A_s B_p - \sum_{s \neq \tilde{s}} \frac{J}{|r_s - r_{\tilde{s}}|^\zeta} A_s A_{\tilde{s}} - \sum_{p \neq \tilde{p}} \frac{J}{|r_p - r_{\tilde{p}}|^\zeta} B_p B_{\tilde{p}} - g_s \sum_s A_s - g_p \sum_p B_p. \quad (27)$$

Once again, when $g_s, g_p, J > 0$, this quantum model shares a ground-state space with the TC. Excited eigenstates of H_{LRSP} are in a one-to-one correspondence with those of the TC albeit with different energy penalties. Pairs of anyons in this model will experience string tension described by the long-range Ising model of H_{LRI} .

FRUSTRATED TOPOLOGICAL ORDER

In the main text, we emphasized the $J > 0, g > 0$ form the SPPM, in which the ground-state space corresponds to ferromagnetic ground-state in the classical model. When $J < 0$ and $g > 0$, the classical model exhibits an antiferromagnetic ground-state when $J < -g/4$. The line $J = -g/4$ then describes the boundary between ferromagnetic and antiferromagnetic phases. In the main text we illustrated that each classical spin configuration corresponds to a d_{TC} -dimensional sector of the SPPM. In this way, the Néel state dual sectors together form the space

$$\mathcal{H}_{\text{Néel}} = \left\{ |\psi\rangle ; A_s B_p |\psi\rangle = -|\psi\rangle \right\}. \quad (28)$$

This sector can be constructed by operating on ferromagnetic spaces $\mathcal{H}_{\text{Ferro+}}$ or $\mathcal{H}_{\text{Ferro-}}$ with one of the following operators.

$$X_{\text{Néel}} = \prod_p X_{\tilde{p},p}^q \quad (29)$$

$$Z_{\text{Néel}} = \prod_s Z_{\tilde{s},s}^q. \quad (30)$$

The operator \mathcal{U}_{sp} of Eq. 22 then connects Néel state dual sectors while preserving topological winding numbers associated to the symmetries of Eq. 4 and Fig. 2. The product of X_N and Z_N is \mathcal{U}_{sp} . Two subspaces of V_N can be identified by the value of A_0 , (in principle an arbitrary star but we take it at the origin as in the previous subsection) which we write as

$$\mathcal{H}_{\text{Néel-}} = \left\{ |\psi\rangle ; A_s B_p |\psi\rangle = A_0 |\psi\rangle = -|\psi\rangle \right\} \quad (31)$$

$$\mathcal{H}_{\text{Néel+}} = \left\{ |\psi\rangle ; A_s B_p |\psi\rangle = -A_0 |\psi\rangle = -|\psi\rangle \right\}. \quad (32)$$

Not all $\{(J_{sp} A_s B_p)\}$ terms in the Hamiltonian can be simultaneously minimized (so as to yield a “frustration free” system). This may not be possible for certain lattices as is easily demonstrated by the duality of Eq. (7) to a frustrated classical model to generate a quantum plaquette/star model counterpart. We may interpret such a frustration as a modification on the typical TC model in which anyons occur in even pairs (or fused products with the total number of generating anyons still even). If we impose periodic boundary conditions on the classical clock model, frustration may occur along either identified boundary, depending on if L_1, L_2 are even or odd. This may be resolved by twisting the boundary conditions and attaching a minus sign to J along the frustrated boundary.

Star-Star and Plaquette-Plaquette Coupling

The simplest case in which the lowest-energy excitations have altered braiding statistics is evident if we introduce the coupling to be between stars and plaquettes. When $q = 2$ (the Ising case), the corresponding Hamiltonian reads

$$H_{ss,pp} = J \sum_{\langle s,s' \rangle} A_s A_{s'} - J \sum_{\langle p,p' \rangle} B_p B_{p'} - g \sum_s A_s - g \sum_p B_p. \quad (33)$$

Note that nearest neighbor star (or plaquette) operators share a common lattice link. Applying Eq. (7), it is seen that this Hamiltonian is dual to a pair of decoupled 2d Ising models. The lowest excitations of this model for $J, g > 0$ are the bound (ee) and (mm) anyon pairs created by applying a single Z link operator (whence the two stars sharing that link are populated by e charge) or single X link operator (creating m charges on the two on plaquettes sharing the link) the ground-state respectively. Splitting these pairs increases associated domain wall energy contributions by $4J$. When $q = 2$, bound pairs braid trivially with one another, and have trivial winding numbers, unlike the free anyons.

STRING-NET MODELS AND QUANTUM DOUBLES

Our illustration that a TQO system (the planar SPPM) is dual to a Landau type theory (the classical clock model) can be readily extended to many other models. We mention a few of these below. String-Net (SN) models use fusion category inputs to construct models on trivalent lattices [10]. Analogous to the TC model, the SN Hamiltonians may be expressed as sums of star and plaquette type operators, $H_{\text{SN}} = -\sum_s A_s^{\text{SN}} - \sum_p B_p^{\text{SN}}$.

The star operator A^{SN} projects states of links sharing a common endpoint onto a space of allowed link configurations while B_p^{SN} transforms link configurations. The definitions of B_p^{SN} are given in terms of nontrivial F -symbols describing the transformations at each vertex [11]. We propose extensions of SN models that include $A_s^{\text{SN}}B_p^{\text{SN}}$ terms, as in Eq. (2), capturing nearest-neighbor anyon interactions. Again, this geometrical dependence has no TQFT description and can be understood through dualities to classical systems. We treat Quantum Double models, which map to a subclass of SN models [12]. We specifically consider the \mathbb{Z}_q Quantum Double Hamiltonian [13],

$$H_{\text{QD}} = - \sum_s A_s^{\text{QD}} - \sum_p B_p^{\text{QD}}, \quad (34)$$

(where $A_s^{\text{QD}} = \sum_{r=0}^{q-1} A_s^r$ and $B_p^{\text{QD}} = \sum_{r=0}^{q-1} B_p^r$ are sums through all powers of the \mathbb{Z}_q TC A_s and B_p operators) and its extension

$$H_{\text{SPQD}} = -J \sum_{\langle s, p \rangle} A_s^{\text{QD}} B_p^{\text{QD}} - g \sum_s A_s^{\text{QD}} - g \sum_p B_p^{\text{QD}}. \quad (35)$$

Repeating, the mapping of Eq. (7) transforms the string-net operators to geometric series of the classical clock spin variables and vice versa, $A_s^{\text{QD}} \leftrightarrow \sum_{r=0}^{q-1} z_i^r$ and $B_p^{\text{QD}} \leftrightarrow \sum_{r=0}^{q-1} (z_j^r)^*$, leading to an unconventional classical clock model that is dual to H_{SPQD} . The possibility of a star-plaquette coupling in quantum double models was also mentioned in [52], where such coupling may introduce tunable anyon masses.

For simplicity of notation, in what follows henceforth, we omit the superscript ‘‘SN.’’ If the trivalent lattice three link labels connected to vertex s are in the state $|ijk\rangle$, then $A_s |ijk\rangle = \delta_{ijk} A_s$ with $\delta_{ijk} = 1$ for allowed vertex states and 0 for not allowed states. B_p is then a linear combination of transforms B_p^w

$$B_p = \sum_s \sum_w a_w B_p^w. \quad (36)$$

The B_p^w are associated to a transformation at each vertex on a plaquette. A geometric interpretation is that B_p^w multiplies each plaquette with an w -th oriented string loop. This view is sometimes called the ‘‘fat lattice construction’’ [7]. The orientation dependence of these loops immediately gives the global constraint $\prod_p B_p^w = 1, \forall w$. Consider a hexagonal plaquette state $|\psi_{abcdef}^{ghijkl}\rangle$ (and legs) with leg links a, b, c, d, e, f and inner plaquette links g, h, i, j, k, l such that a forms a star with g and h , b with h and i , etc.,

$$B_p^w |\psi_p\rangle = \sum_{g' h' i, \dots} B_{p,ghi\dots}^{w,g'h'i\dots} (abcdef) |\psi_{abcdef}^{g'h'i'j'k'l'}\rangle. \quad (37)$$

A single such term is then described by 6 index F -symbols associated to each vertex transformation,

$$\begin{aligned} B_{p,ghi\dots}^{w,g'h'i\dots} (abcdef) &= F_{w^*g'l'^*}^{al^*g} F_{w^*h'g'^*}^{bg^*h} F_{w^*i'h'^*}^{ch^*i} \\ &\times F_{w^*j'i'^*}^{di^*j} F_{w^*k'j'^*}^{ej^*k} F_{w^*l'k'^*}^{fk^*l}. \end{aligned} \quad (38)$$

Each F -symbol obeys a series of constraints and defines the rules of allowed link combinations [11]. It should be noted that explicit partition functions and spectra of these models have been studied in [53, 54], which must ultimately play into our extensions.

The operators B_p^w and A_s commute by construction, supplementing Eq. (5a). Constraints on B_p^w operators, analogous to Eq. 5b, are then realized through the underlying group structure of B_p^w . A global constraint like Eq. 5d is, again, established for B_p^w by the aforementioned ‘‘fat lattice’’ construction. We can map the B_p^w operators into site-local degrees of freedom representing the same group, such as we had in the SPPM for classical clocks. Extending these types of constraints to string-net A_s terms or some decomposition of some A_s^u , similar to B_p^w , would allow us to directly relate many string-nets to classical models. We could then finally establish constraints on bilinear strings of A_s^u and B_p^w operators of the same type as Eq. 5c. Quantum double models are a simple example of this, in the sense of their mapping to both string-nets and classical models. Further difficulties arise when F -symbols introduce complex phases, such as the \mathbb{Z}_2 Chern-Simons phase in [11]. In this, plaquettes also include complex phase factors on the legs which can be factored out of B_p^w . Remaining terms are mapped to classical degrees of freedom. The TQFT then used as the low energy effective theory is a $U(1) \times U(1)$ Chern-Simons theory. Additional coupling, just as in the SPPM, can change the nature of lowest-energy excitations without changing the ground-state space.

HIGHER-DIMENSIONAL MODELS

Higher-dimensional systems dual to clock models can be constructed from extensions of known stabilizer models. For instance, we may map an SPPM type extension of the cubic lattice \mathbb{Z}_q TC model [30, 43, 55] to a classical clock model on the face-centered cubic lattice (FCC) as shown in Fig. 4. This model obeys Eqs. 5a-5d. We define it by Eq. (2) yet now with six spin star $A_s = \prod_{j \in s} X_j$ and four spin plaquette $B_p = Z_1 Z_2^\dagger Z_3 Z_4^\dagger$ operators (with indexing, once again, performed anti-clockwise) as depicted in Fig. 4. In this variant of Eq. (2) the nearest-neighbor condition $\langle s, p \rangle$ is defined on the 3D cubic lattice. We map each face B_p to a z_j^* at the center of an FCC face. The star operators A_s at the cubic lattice sites are mapped to z_j lying on FCC cube corners (Fig 4). Cubic lattice TC models display TQOs which are

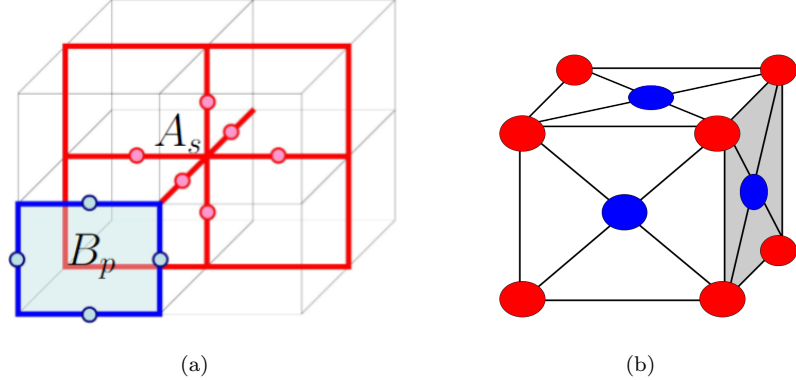


FIG. 4: (Color online.) (a) Red circled links form a 3D toric code [43] star while circled blue links form a 3D plaquette. (b) A cubic cell of the FCC. Plaquette operators map into blue vertex clocks on FCC faces. Star operators map to red vertex clocks on FCC corners.

membrane extensions of string order seen in the (2+1)D

case [30, 43, 55]. In [9], we discuss *string-net model* extensions that exhibit similar behaviors.